

A Determination of the Intergalactic Redshift Dependent UV-Optical-NIR Photon Density Using Deep Galaxy Survey Data and the Gamma-ray Opacity of the Universe

Floyd W. Stecker

Astrophysics Science Division, NASA/Goddard Space Flight Center

Department of Physics and Astronomy, University of California, Los Angeles

Matthew A. Malkan

Department of Physics and Astronomy, University of California, Los Angeles

Sean T. Scully

Department of Physics, James Madison University

Received _____; accepted _____

ABSTRACT

We calculate the intensity and photon spectrum of the intergalactic background light (IBL) as a function of redshift using an approach based on observational data obtained at in different wavelength bands from local to deep galaxy surveys. Our empirically based approach allows us, for the first time, to obtain a completely model independent determination of the IBL and to quantify its uncertainties. Using our results on the IBL, we then place 68% confidence upper and lower limits on the opacity of the universe to γ -rays , independent of previous constraints that were obtained by making theoretical assumptions. We then compare our results with measurements of the extragalactic background light and upper limits obtained from observations made by the *Fermi* Gamma-ray Space Telescope.

Subject headings: diffuse radiation – galaxies:observations – gamma rays:theory

1. Introduction

1.1. Empirical Approach to Determining the Intergalactic Background Radiation

In this paper we explore a new fully empirical approach to calculating the intergalactic background light (IBL) as well as the γ -ray opacity of the Universe. This approach, hitherto unavailable, is now enabled by very recent data from deep galaxy surveys spanning the electromagnetic spectrum from millimeter to UV wavelengths and using galaxy luminosity functions for redshifts $0 \leq z \leq 8$. We stress that our empirical approach is the first ever study that is *totally model independent*. It is also the first approach capable of *delineating*

empirically based uncertainties on the determination of the IBL, something that previous model-based approaches could not do.

The determination of the local IBL at $z = 0$, also known as the extragalactic background light (EBL), has been of particular interest and will be addressed here. Our $z = 0$ EBL results will be compared with background measurements and lower limits from galaxy counts. In this paper (Paper I) we specifically consider the frequency range from the far ultraviolet (FUV) to the near infrared I band (NIR), as this range is of particular relevance to the γ -ray opacity studies in the ~ 0.1 -200 GeV energy range being made by the *Fermi* γ -ray space telescope. A follow-up paper (Paper II) will address the frequency range from the NIR to the far-IR (FIR). That range has particular relevance for opacity studies by ground-based air Čerenkov telescopes.

Previous approaches to calculate the IBL at different redshifts, corresponding to different cosmological epochs, have required various theoretical models and assumptions. These approaches include backward evolution models (Malkan & Stecker 1998, 2001; Stecker, Malkan & Scully 2006; Franceschini et al. 2008), semi-analytical forward evolution models (*e.g.*, Gilmore et al. 2009; Somerville et al. 2011) and other models based on the evolution of galaxy parameters such as star formation rate and stellar population synthesis models (Salamon & Stecker 1998; Kneiske et al. 2004). Kneiske & Dole (2010) have recently used a forward evolution model to derive lower limits on the EBL. The exploration of the EBL using direct measurements, galaxy counts, and indirect constraints has been reviewed by Hauser & Dwek (2001).

Our estimates of the low energy background photons produced by galaxies at all redshifts will have several key advantages over any previous work. Previous studies had to adopt assumptions about how the galaxy luminosity function (LF) evolves with cosmic time, starting either at the present (well-measured epoch) and going back in time, or

starting with the simulations of the galaxy formation epoch using semi-analytic models (see above). However, the latest observations have finally become sufficiently extensive and accurate to replace these approaches with a *direct integration* of observational data on galaxy LFs from the deep galaxy surveys, where we can smoothly interpolate between observationally determined LFs in each redshift range from $z = 0$ to $z \geq 8$.

Thus, the first goal of our paper is to determine the IBL based on empirical data from deep survey galaxy observations. Our empirically based approach avoids the complications entailed by theoretical calculations that have need of making various assumptions for stellar population synthesis models, unknown amounts of dust extinction, and poorly known stellar metallicity-age modeling for different evolving galaxy types.

1.2. Gamma Ray Opacity and the IBL

The second goal of our paper is to use our results on the IBL to determine the γ -ray opacity of the universe as a function of energy and redshift. It was first suggested by Stecker, De Jager & Salamon (1992) that γ -ray observations from high redshift sources such as blazars (and later γ -ray bursts) could be used to probe the IBL. Such studies make use of the opacity caused by the annihilation of γ -rays owing to interactions with low energy photons that produce e^+e^- pairs. The *Fermi Gamma-Ray Space Telescope (Fermi)* is now being used to probe the high redshift IBL at optical and UV wavelengths by constraining the opacity of the universe to multi-GeV γ -rays (Abdo et al. 2010). This is accomplished by measuring the energy of the highest energy photons observed by *Fermi* that have been emitted by GRBs and blazars at known redshifts.

Observations of TeV γ -ray emitting blazars utilizing modern air Čerenkov telescope arrays also probe, or at least constrain, the nearby (redshift $z \sim 0 - 0.5$) intergalactic

infrared background radiation. Attempts to constrain the EBL have been made by various authors (Stecker & de Jager 1993; Aharonian et al. 2006 (but see Stecker, Baring & Summerlin 2009); Mazin & Raue 2007; Georganopoulos, Fincke & Reyes 2010; Abdo et al. 2010; Orr, Krennrich & Dwek 2011, but see Stecker, Baring & Summerlin 2009).

Our new approach will also be used to empirically define a secure lower limit and an upper limit for the opacity of the universe to high energy γ -rays using deep survey data. We then compare the opacity range defined by these limits with the upper limits derived using the *Fermi* observations of multi-GeV γ -rays from high redshift sources Abdo, et al (2010).

2. Intergalactic Photon Energy Densities and Emissivities from Galaxies

The co-moving radiation energy density $u_\nu(z)$ is derived from the co-moving specific emissivity $\mathcal{E}_\nu(z)$, which, in turn is derived from the galaxy luminosity function (LF). The galaxy luminosity function, $\Phi_\nu(L)$, is defined as the distribution function of galaxy luminosities at a specific frequency or wavelength. The specific emissivity at frequency ν and redshift z (also referred to in the literature as the luminosity density, ρ_{L_ν}) , is the integral over the luminosity function

$$\mathcal{E}_\nu(z) = \int_{L_{min}}^{L_{max}} dL_\nu \Phi(L_\nu; z) \quad (1)$$

There are many references in the literature where the LF is given and fit to Schechter parameters, but where ρ_{L_ν} is not given. In those cases, we could not determine the covariance of the errors in the Schechter parameters and therefore could not determine the error on the emissivity from equation (1). We therefore chose to use only the papers that gave values for $\rho_{L_\nu}(z) = \mathcal{E}_\nu(z)$ with errors. We did not consider cosmic variance, but this uncertainty should be minimized since we used data from many surveys.

In compiling the observational data on $\mathcal{E}_\nu(z)$, we scaled all of the results to a value of $h = 0.7$. Thus results using $h = 0.5$ were scaled by a factor of $(7/5)$.

The co-moving radiation energy density $u_\nu(z)$ is the time integral of the co-moving specific emissivity $\mathcal{E}_\nu(z)$,

$$u_\nu(z) = \int_z^{z_{\max}} dz' \mathcal{E}_{\nu'}(z') \frac{dt}{dz}(z') e^{-\tau_{\text{eff}}(\nu, z, z')}, \quad (2)$$

where $\nu' = \nu(1 + z')/(1 + z)$ and z_{\max} is the redshift corresponding to initial galaxy formation (Salamon & Stecker 1998, hereafter SS98), and

$$\frac{dt}{dz}(z) = [H_0(1 + z)\sqrt{\Omega_\Lambda + \Omega_m(1 + z)^3}]^{-1}, \quad (3)$$

with $\Omega_\Lambda = 0.72$ and $\Omega_m = 0.28$.

The opacity factor for frequencies below the Lyman limit is dominated by dust extinction. In the model of SS98, which relied on the population synthesis studies of Bruzual & Charlot (1993), dust absorption was not included. Our earlier paper (Stecker, Malkan & Scully 2006) used a rough approximation of the results obtained by Salamon & Stecker (1998) (hereafter SS98) and therefore, also did not take dust absorption into account. However, since we are here using actual observations of galaxies rather than models, dust absorption is implicitly included. The remaining opacity τ_ν refers to the extinction of ionizing photons with frequencies above the rest frame Lyman limit of $\nu_{LyL} \equiv 3.29 \times 10^{15}$ Hz by interstellar and intergalactic hydrogen and helium. It has been shown that this opacity is very high, corresponding to the expectation of very small fraction of ionizing radiation in intergalactic space compared with radiation below the Lyman limit (Lytherer et al.1995; SS98). In fact, the Lyman limit cutoff is used as a tool; when galaxies disappear when using a filter at a given waveband (*e.g.*, "U-dropouts", "V-dropouts") it is an indication of the redshift of the Lyman limit.

We thus replace equation (2) with the following expression

$$u_\nu(z) = \int_z^{z_{\max}} dz' \mathcal{E}_\nu(z') \frac{dt}{dz}(z') \mathcal{H}(\nu(z') - \nu'_{LyL}), \quad (4)$$

where $\mathcal{H}(x)$ is the Heavyside step function.

2.1. Empirical Specific Emissivities

2.1.1. Luminosity Densities

We have used the results of many galaxy surveys to compile a set of luminosity densities, $\rho_{L\nu}(z) = \mathcal{E}_\nu(z)$ (LDs), at all observed redshifts, and at rest-frame wavelengths from the far-ultraviolet, FUV = 150 nm to the I band, $I = 800$ nm. The LDs were obtained with a wide variety of instruments in many different deep fields¹

¹References for the values of $\mathcal{E}_\nu(z)$ used to construct Figure 1 are as follows: FUV band: Steidel et al.(1999), Budavári et al.(2005), Schiminovich et al.(2005), Wyder et al.(2005), Sawicki & Thompson (2006), Yoshida et al.(2006), Bouwens et al.(2007), Burgarella et al.(2007), Dahlen et al.(2007), Iwata et al.(2007), Paltani et al.(2007), Tresse et al.(2007), Reddy et al.(2008), Ly et al.(2009), Reddy & Steidel (2009), Bouwens et al.(2010), Oesch et al.(2010), Bouwens et al.(2011a), Robotham & Driver (2011), Cucciati et al.(2012) NUV band: Budavári et al.(2005), Wyder et al.(2005), Dahlen et al.(2007), Tresse et al.(2007), Robotham & Driver (2011), U band: Dahlen et al.(2005), Tresse et al.(2007), B band: Dahlen et al.(2005), Faber et al.(2007), Marchesini et al.(2007), Tresse et al.(2007), Bouwens et al.(2011a), V band: Marchesini et al.(2007), Tresse et al.(2007), Bouwens et al.(2011a), Marchesini et al.(2012), R band: Chen et al.(2003), Dahlen et al.(2005), Marchesini et al.(2007), Tresse et al.(2007), I band: Tresse et al.(2007), Bouwens et al.(2011a).

Figure 1 shows the redshift evolution of the luminosity density for the various wavebands based on those published in the literature and our color relations as described in the next subsection.

It is hardly surprising that there are often large apparent jumps, or changes, in the shape and the normalization of the LDs going from one waveband to an immediately adjacent one. We therefore applied a second test of the consistency of these LDs, by comparing the integrated *ratios* of LDs at adjacent wavebands to the published average colors measured by observers. This test has the great advantage of not requiring accurate estimates of volume incompleteness or even very accurate redshifts. Broadband colors (*i.e.*, local continuum slopes) are easier to measure than LDs. The main problem is that all galaxy samples at all redshifts show a wide observed range of broadband colors. The typical 1σ scatter we found in published color distributions was ± 0.5 mag. A few rest-frame colors that are very sensitive to stellar population, such as $U - B$, often show even larger variation.

In order to then determine the redshift evolution of the LD in each of the bands all the way out to a redshift of ~ 8 , we utilized color relations to transform data from other bands. We have chosen to include all data possible in excess of $z = 1.5$ to fill in the gaps for various wavebands mostly at higher redshifts. This also provides both an overlap to existing data and multiple sources of data as a check for consistency of our color relations.

2.1.2. Average Colors

Published estimates of *average colors* from galaxy surveys at various wavebands and redshifts tend to be bluer at shorter wavelengths, and redder at longer wavelengths. This is due to the composite nature of stellar populations in galaxies, with hot young stars making a stronger contribution in the UV portion of the spectrum while red giants dominate the

long wavelengths. Thus, the galaxies that are included in a UV LF and not all the same galaxies as those included in an LF in the R band.

There is a clear trend with redshift over all wavelengths, which is well known. Redder galaxies (*e.g.*, local E and S0 galaxies) are more and more outnumbered by blue, actively star-forming galaxies, at higher redshifts. The average characteristic age of stellar populations decreases with redshift and our color relations agree with this trend. At the highest redshifts most known galaxies are dominated by young starburst populations of O and B stars, which tends to produce very blue overall spectral energy distribution without very much sensitivity to the exact details of the star formation. These factors are automatically taken into account when one uses the actual observational data on the LDs at various wavelengths and redshifts.

Defining the average wavelengths of the various bands in nm as follows:

$$FUV = 150, NUV = 280, U = 365, B = 445, V = 551, R = 658, I = 806 \text{ nm}$$

We then use the commonly measured astronomical parameter β , which is defined by the relation between the differential flux and wavelength of a galaxy, $f_\lambda \propto \lambda^\beta$. We have adopted the following relations (colors) for $\beta_{\Delta\lambda}(z)$:

$$\beta(FUV - NUV) = -1.0 - 1.25\log(1 + z), \log(1 + z) \leq 0.8$$

derived from Bouwens, et al. (2009); Budavári et al.(2005); Castellano et al. (2012); Cucciati, et al. (2012); Dunlop et al. (2012); Willott, et al. (2012); Wyder et al.(2005),

$$\beta(B - V) = +0.3 - 1.6\log(1 + z), \log(1 + z) \leq 0.6$$

derived from Arnouts et al.(2007); Brammer (2011),

$$\beta(NUV - U) = +0.5 - 1.2\log(1 + z), \log(1 + z) \leq 0.6$$

derived from Tresse et al. (2007),

$$\beta(NUV - R) = +2.5 - 6.0 \log(1 + z), \log(1 + z) \leq 0.6$$

$$\beta(U - V) = +1.3 - 3.0 \log(1 + z), \log(1 + z) \leq 0.6$$

derived from Arnouts, et al. (2007); Brammer (2011); Ly et al. (2009),

$$\beta(U - B) = +3.0 - 5.0 \log(1 + z), \log(1 + z) \leq 0.6$$

derived from Marchesini et al. (2007); González et al. (2011),

For the FUV-NUV relation we set $\beta[\log(1 + z) > 0.8] = \beta[\log(0.8)]$. For all of the other relations we set $\beta[\log(1 + z) > 0.6] = \beta[\log(0.6)]$.

2.2. Photon Density Calculations

The observationally determined LDs, combined with the color relations, extend our coverage of galaxy photon production from the FUV to the NIR in the galaxy rest frame. We have at least one or two determinations at each wavelength across the most crucial redshift range $0 \leq z \leq 2.5$. However, to calculate the opacity for photons at energies higher than $\sim 250/(1 + z)$ GeV (see next section), requires the determination of galaxy LDs at longer rest wavelengths and higher redshifts. These regimes are less well constrained by observations, since they require measurement of very faint galaxies at long wavelengths (mid-IR observed frame.) We will address this topic in Paper II. We have assumed a constant color at high redshift at the longer wavelengths as stated above. However, we stress that our final results are not very sensitive to errors in our average color relations because the interpolations that we make cover very small fractional wavelength intervals, $\Delta\lambda(z)$.

The second goal of our paper is to place upper and lower limits (within a 68% confidence band) on the opacity of the universe to γ -rays . These limits are a direct result of the 68% confidence band upper and lower limits of the IBL determined from the observational data on $\rho_{L\nu}$. In order to determine these limits, we make no assumptions about the luminosity density evolution. We derive a luminosity confidence band in each waveband by using a robust rational fitting function characterized by

$$\rho_{L\nu} = \mathcal{E}_\nu(z) = \frac{ax + b}{cx^2 + dx + e} \quad (5)$$

where $x = \log(1 + z)$ and $a, b, c, d,$ and e are free parameters.

The 68% confidence band is then computed from Monte Carlo simulation by finding 100,000 realizations of the data and then fitting the rational function. In order to best represent the tolerated confidence band, particularly at the highest redshifts, we have chosen to equally weight all FUV points in excess of a redshift of 2. Our goal is not to find the best fit to the data but rather the limits tolerated by the current observational data. In order to perform the Monte Carlo of the fitting function, a likelihood is determined at each redshift containing data. The shape of the function is taken to be Gaussian (or the sum of Gaussians where multiple points exist) for symmetric errors quoted in the literature. Where symmetric errors are not quoted it is impossible to know what the actual shape of the likelihood functions is. We have chosen to utilize a skew normal distribution to model asymmetric errors. This assumption has very little impact on the determination of the confidence bands. The resulting bands are shown along with the luminosity density data in Figure 1.

With the confidence bands established, we take the upper and lower limits of the bands to be our high and low IBL respectively. We then interpolate each of these cases separately between the various wavebands to find the upper and lower limit rest frame luminosity densities. The calculation is extended to the Lyman limit using the slope derived from our

color relationship between the near and far UV bands.

The specific emissivity is then the derived high and low IBL luminosity densities $\mathcal{E}_\nu(z) = \rho_{L_\nu}(z)$. The co-moving radiation energy density is determined from equation 4. Figure 2 shows the resulting photon density determined by dividing the energy density by the energy in each frequency for high and low IBL. This result is used as input for the determination of the optical depth of the universe to γ -rays .

The photon densities

$$\epsilon n(\epsilon, z) = u(\epsilon, z)/\epsilon \quad , \quad (6)$$

with $\epsilon = h\nu$, as calculated using equation (2), are shown in Figure 2.

3. Comparison of $z = 0$ IBL with Data and Constraints

Using equation (2), together with our empirically based determinations of the confidence band of specific emissivities, $\mathcal{E}_\nu(z)$, we have evaluated the spectral energy distribution of the IBL at $z = 0$, commonly known as the extragalactic background light (EBL). This band is indicated by the gray zone in Figure 6. We also show recent measurements using the Hubble Wide-field Planetary Camera 2 (Bernstein 2007), the dark field from Pioneer 10/11 (Matsuoka et al. 2011) and differential measurements using the ESO VLT (very large telescope array) (Mattila et al. 2011). Figure 6 also shows the various lower limits from galaxy counts obtained by Gardener et al. (2000) from the ST Imaging Spectrograph data, by Madau & Pozzetti (2000) using Hubble Deep Field South data, and by Xu et al. (2005) from GALEX (Galaxy Evolution Explorer) data, all indicated by upward-pointing arrows.

Since there is no significant conflict between our determination of the diffuse EBL from unresolved galaxies and the measurements shown in Figure 3, we conclude that there is no

other significant unknown component to the EBL.

4. The Optical Depth from Interactions with Intergalactic Low Energy Photons

The cross section for photon-photon scattering to electron-positron pairs can be calculated using quantum electrodynamics (Breit & Wheeler 1934). The threshold for this interaction is determined from the frame invariance of the square of the four-momentum vector that reduces to the square of the threshold energy, s , required to produce twice the electron rest mass in the c.m.s.:

$$s = 2\epsilon E_\gamma(1 - \cos \theta) = 4m_e^2 \quad (7)$$

This invariance is known to hold to within one part in 10^{15} (Stecker & Glashow 2001; Jacobson, Liberati, Mattingly & Stecker 2004).

With the co-moving energy density $u_\nu(z)$ evaluated, the optical depth for γ -rays owing to electron-positron pair production interactions with photons of the stellar radiation background can be determined from the expression (Stecker, De Jager, & Salamon 1992)

$$\tau(E_0, z_e) = c \int_0^{z_e} dz \frac{dt}{dz} \int_0^2 dx \frac{x}{2} \int_0^\infty d\nu (1+z)^3 \left[\frac{u_\nu(z)}{h\nu} \right] \sigma_{\gamma\gamma}[s = 2E_0 h\nu x(1+z)], \quad (8)$$

In equations (7) and (8), E_0 is the observed γ -ray energy at redshift zero, ν is the frequency at redshift z , z_e is the redshift of the γ -ray source at emission, $x = (1 - \cos \theta)$, θ being the angle between the γ -ray and the soft background photon, h is Planck's constant, and the pair production cross section $\sigma_{\gamma\gamma}$ is zero for center-of-mass energy $\sqrt{s} < 2m_e c^2$, m_e being the electron mass. Above this threshold, the pair production cross section is given by

$$\sigma_{\gamma\gamma}(s) = \frac{3}{16}\sigma_T(1 - \beta^2) \left[2\beta(\beta^2 - 2) + (3 - \beta^4) \ln \left(\frac{1 + \beta}{1 - \beta} \right) \right], \quad (9)$$

where σ_T is the Thompson scattering cross section and $\beta = (1 - 4m_e^2c^4/s)^{1/2}$ (Jauch & Rohrlich 1955).

It follows from equation (7) that the pair-production cross section energy has a threshold at $\lambda = 4.75 \mu\text{m} \cdot E_\gamma(\text{TeV})$. Since the maximum λ that we consider here is in the rest frame I band at $790 \pm 75 \text{ nm}$ at redshift z , and we observe E_γ at redshift 0, so that its energy at interaction in the rest frame is $(1 + z)E_\gamma$, we then get a conservative upper limit on E_γ of $\sim 200(1 + z)^{-1} \text{ GeV}$ as the maximum γ -ray energy affected by the photon range considered here. Allowing for a small error, our opacities are good to $\sim 250(1 + z)^{-1} \text{ GeV}$.

The 68% opacity ranges for $z = 0.1, 0.5, 1, 3$ and 5 , calculated using equation (8) are plotted in Figure 4.

The widths of the grey uncertainty ranges in the LDs shown in Figure 1 increase towards higher redshifts, especially at the longest rest wavelengths. This reflects the decreasing amount of long-wavelength data and the corresponding increase in uncertainties about the galaxies in those regimes. However, these uncertainties do not greatly influence the opacity calculations. Because of the short time interval of the emission from galaxies at high redshifts their photons do not contribute greatly to the opacity at lower redshifts, as can be seen from Figure 4.

5. Results and Implications

We have determined the IBL using local and deep galaxy survey data, together with observationally produced uncertainties, for wavelengths from 150 nm to 690 nm and redshifts out to $z > 5$. We have presented our results in terms of 68% confidence band

upper and lower limits. As expected, our lower limits are higher than those obtained by galaxy counts alone, since the IBL from galaxies is not completely resolved. Our results are also above the theoretical lower limits given recently by Kneiske and Dole (2010). In addition, we find that they are compatible with recent measurements reported by Matsuoka et al. (2011) and Mattila et al. (2011).

Figure 5 shows our 68% confidence band for $\tau = 1$ on an energy-redshift plot compared with the *Fermi* data on the highest energy photons from extragalactic sources at various redshifts as given by Abdo et al. (2010). It can be seen that none of the photons from these sources would be expected to be significantly annihilated by pair production interactions with the IBL. This point is brought out further in Figure 6. This figure compares the 68% confidence band of our opacity results with the 95% confidence upper limits on the opacity derived for specific blazars by Abdo et al. (2010).

Our results have important potential implications for probing the potential amount of secondary γ -rays from interactions of high energy protons produced by blazars (Essey et al. 2010; Essey & Kusenko 2012). Our result also bears on the question of whether or not axion-photon oscillations play a role in the propagation of γ -rays from distant extragalactic sources (De Angelis et al. 2009). Future theoretical studies and future γ -ray observations of extragalactic sources with *Fermi* and the *Čerenkov Telescope Array*, which will be sensitive to extragalactic sources at energies above 10 GeV (Gernot 2011), should help to clarify these important aspects of high energy astrophysics.

6. Our Results Online

Our results in numerical form are available at the following link:

<http://csma31.csm.jmu.edu/physics/scully/opacities.html>

Acknowledgments

We would like to thank Luis Reyes and Anita Reimer for supplying us with the Fermi results shown in Figure 5. We thank Richard Henry for a helpful discussion of the UV background data. This research was partially supported by a NASA Astrophysics Theory Grant and a NASA Fermi Guest Investigator Grant.

Figure Captions

Figure 1: The specific emissivities in our fiducial wavebands. The lower right panel shows all of the observational data from the references in footnote 1. In the other panels, non-band data have been shifted using the color relations given in the text in order to fully determine the specific emissivities in each waveband. The symbol designations are FUV:filled circles, NUV:open circles, U :filled squares, B :open squares, V :filled triangles, R :open triangles, I :open diamonds. Grey shading: 68% confidence bands (see text).

Figure 2: The photon densities $\epsilon n(\epsilon)$ shown as a continuous function of photon energy and redshift for both the high (upper panel) and low (lower panel) IBL.

Figure 3: Our empirically-based determination of the EBL together with lower limits and data as described in the text. The legend is as follows: Madau & Pozzetti(2000):Black Cicles, Xu et al.(2005):Crosses, Gardner et al.(2000):Open Squares, Matsuoka et al.(2011):Open Circles, Mattilla et al.(2011):Black Squares, Bernstein(2007):Black Diamonds.

Figure 4: Our empirically determined opacities for redshifts of 0.1, 0.5, 1, 3, 5. The dashed lines are for $\tau = 1$ and $\tau = 3$.

Figure 5: A $\tau = 1$ energy-redshift plot (Fazio & Stecker 1970) showing our uncertainty band results compared with the *Fermi* plot of their highest energy photons from FSRQs (red), BL Lacs (black) and and GRBs (blue) *vs.* redshift (from Abdo et al. 2010).

Figure 6: Our opacity results for the redshifts of the blazars having 95% confidence opacity upper limits given by Fermi (Abdo, et al. 2010).

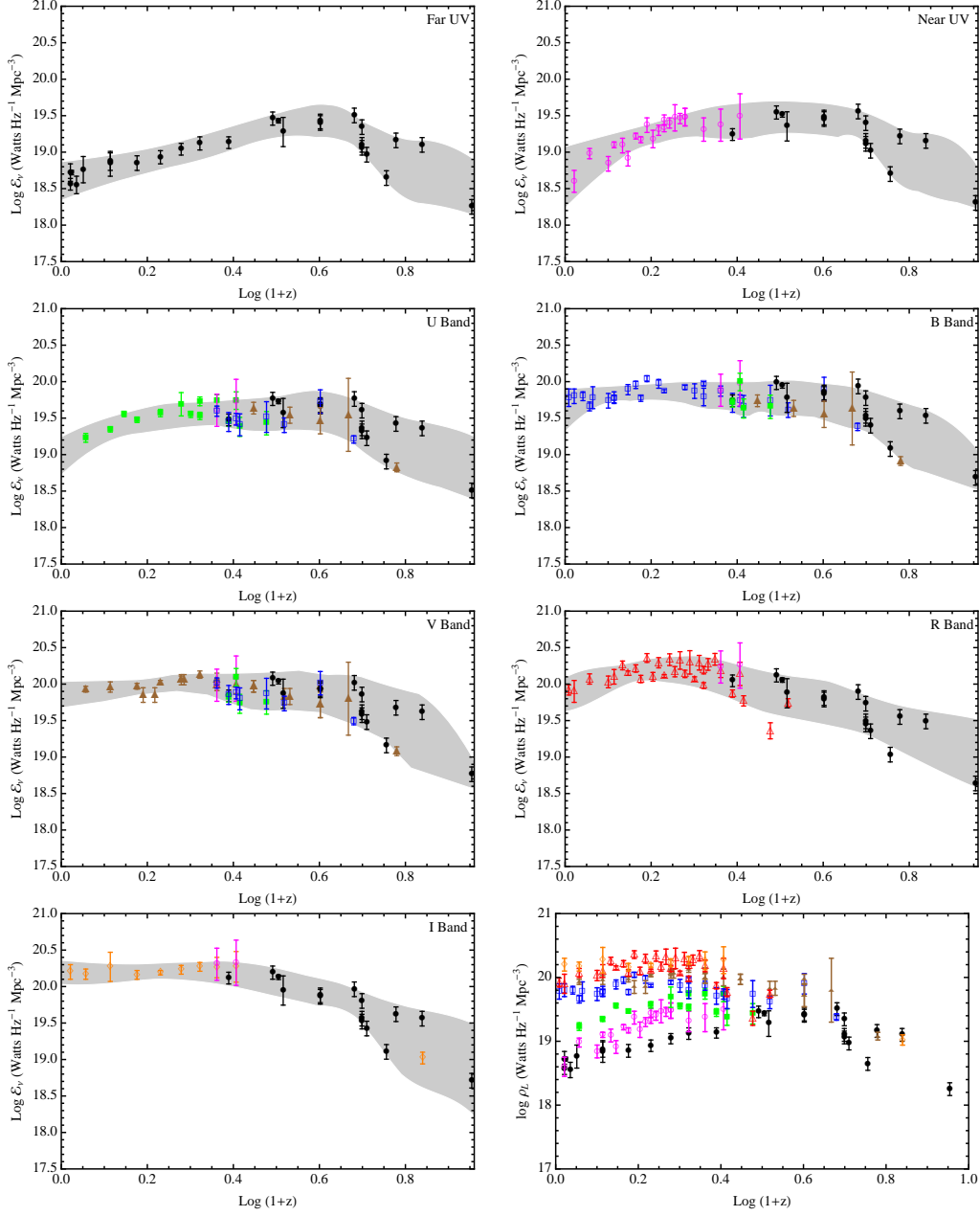


Figure 1.

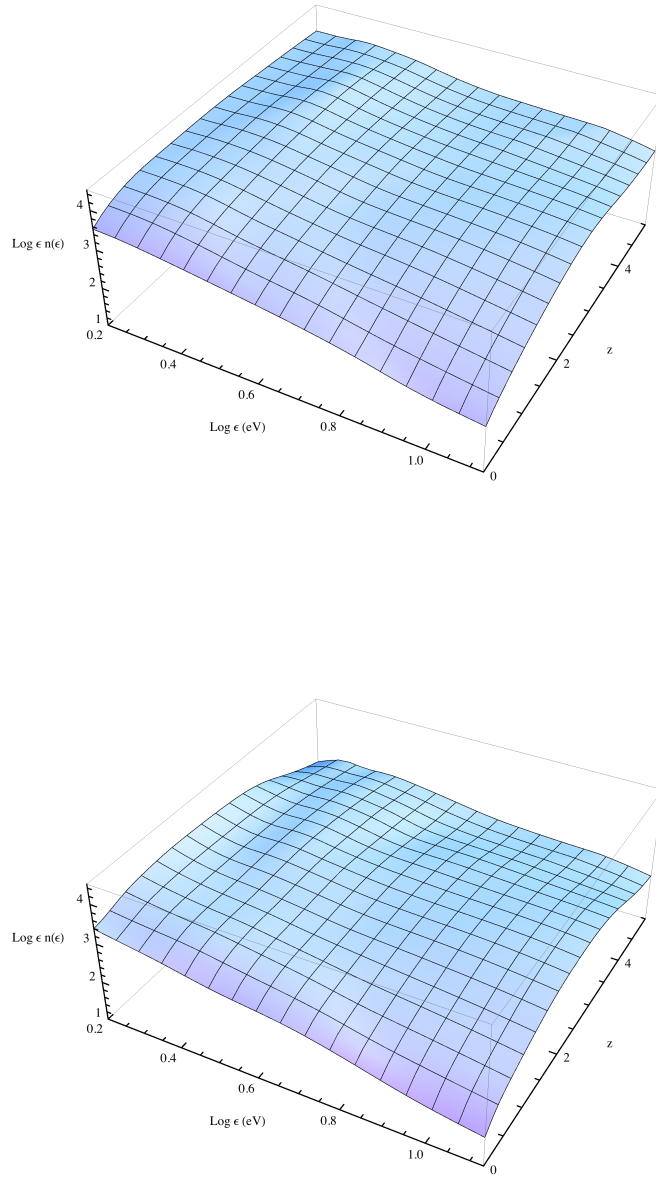


Figure 2.

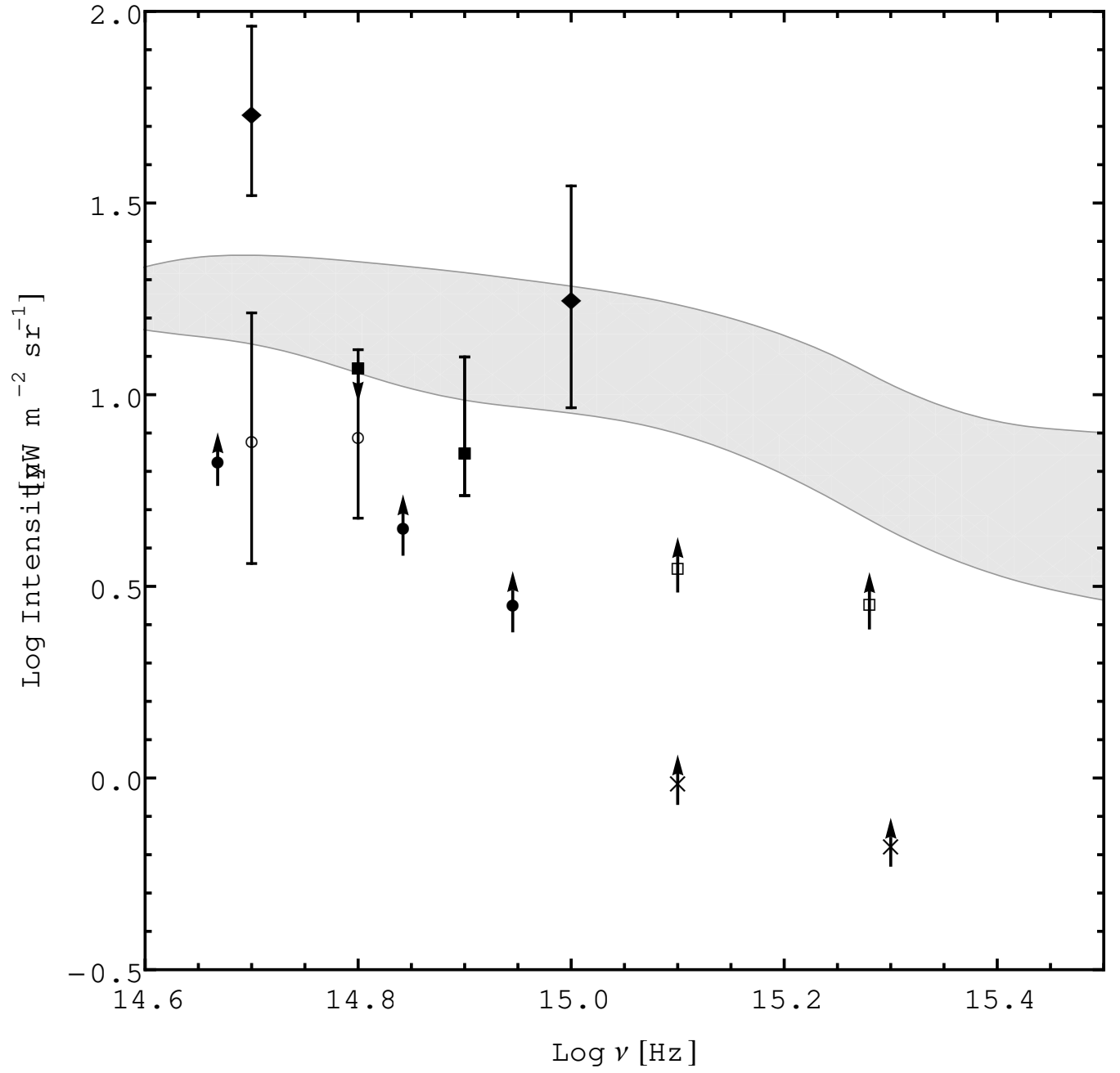


Figure 3.

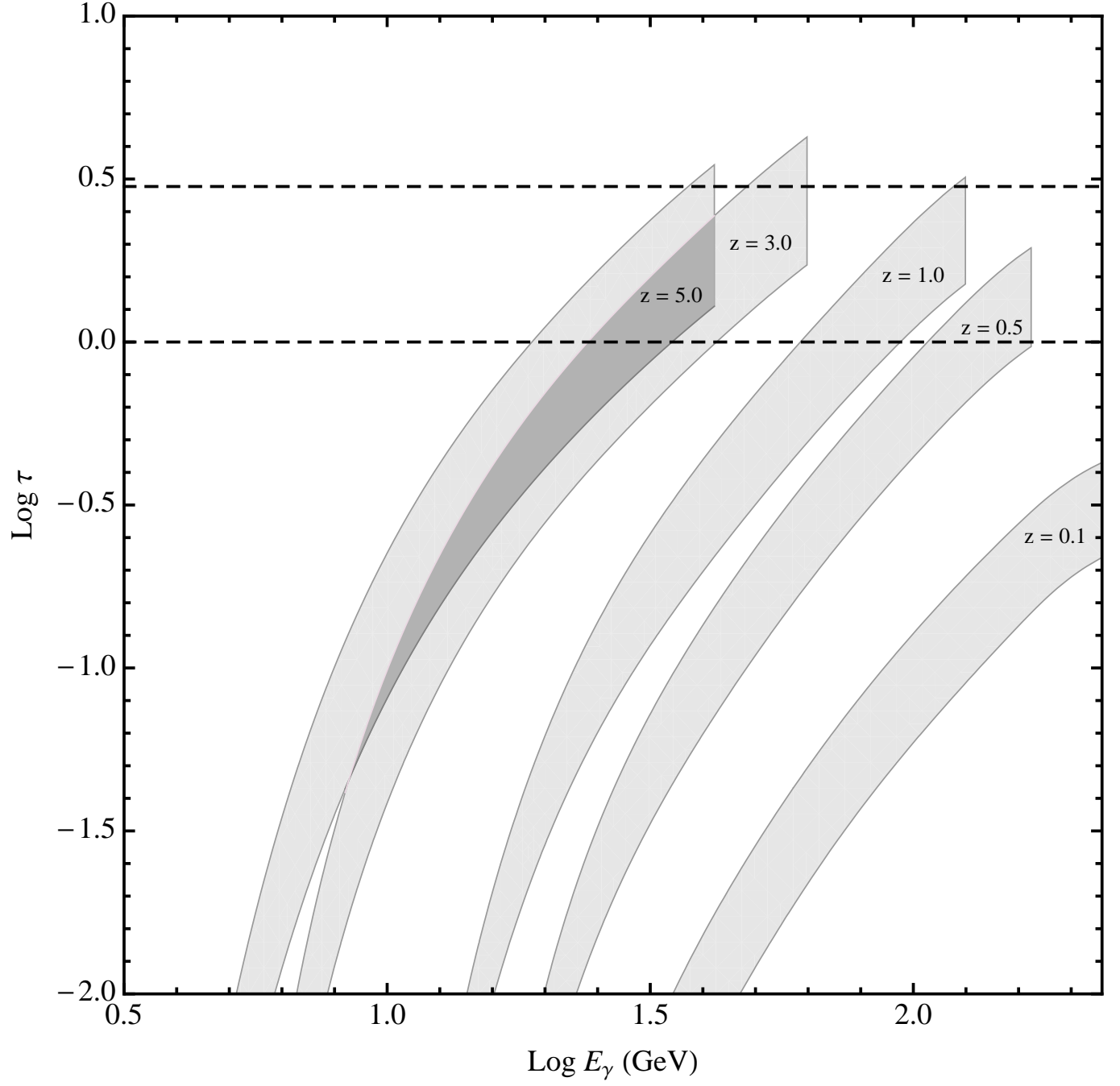


Figure 4.

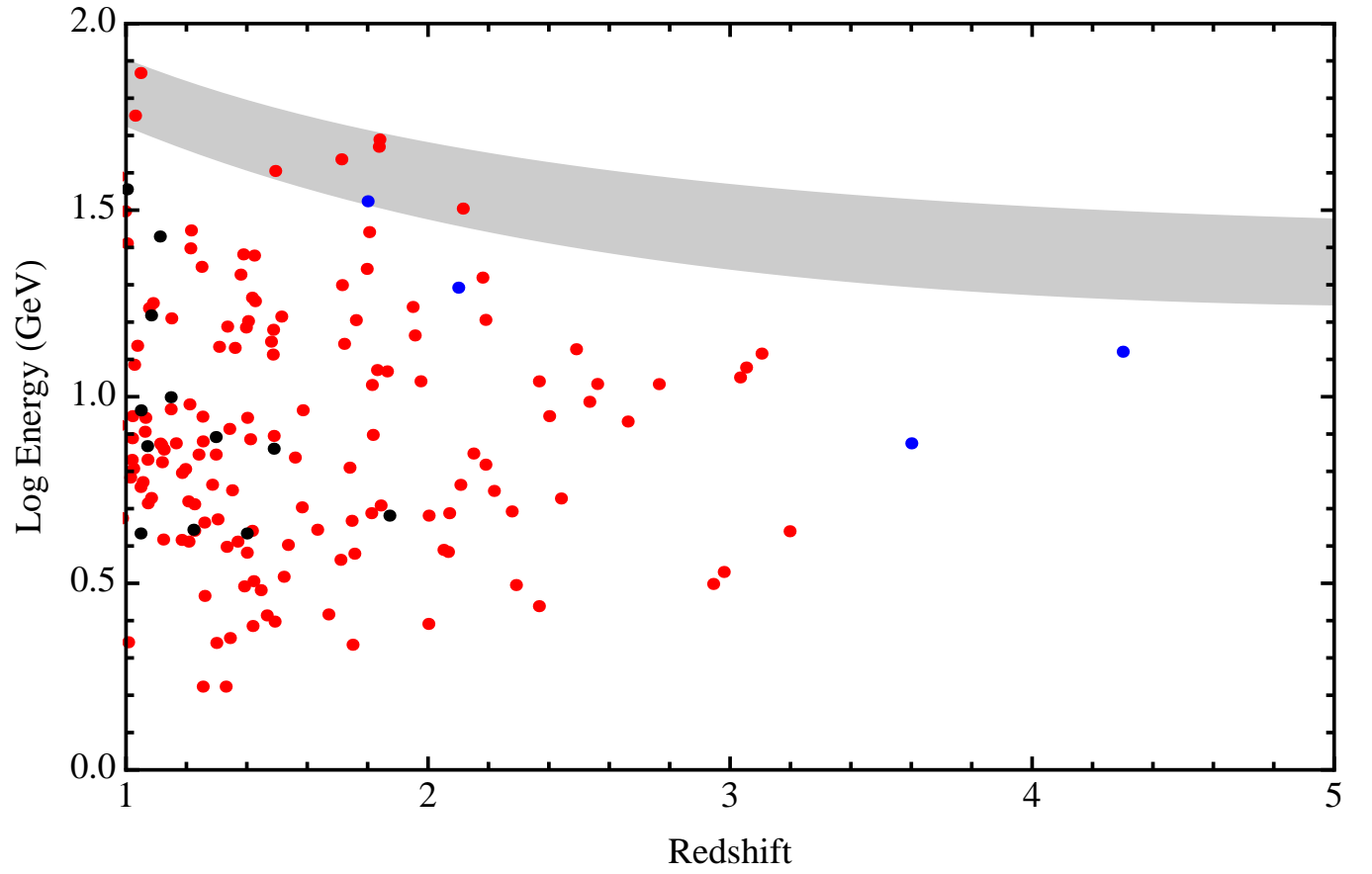


Figure 5.

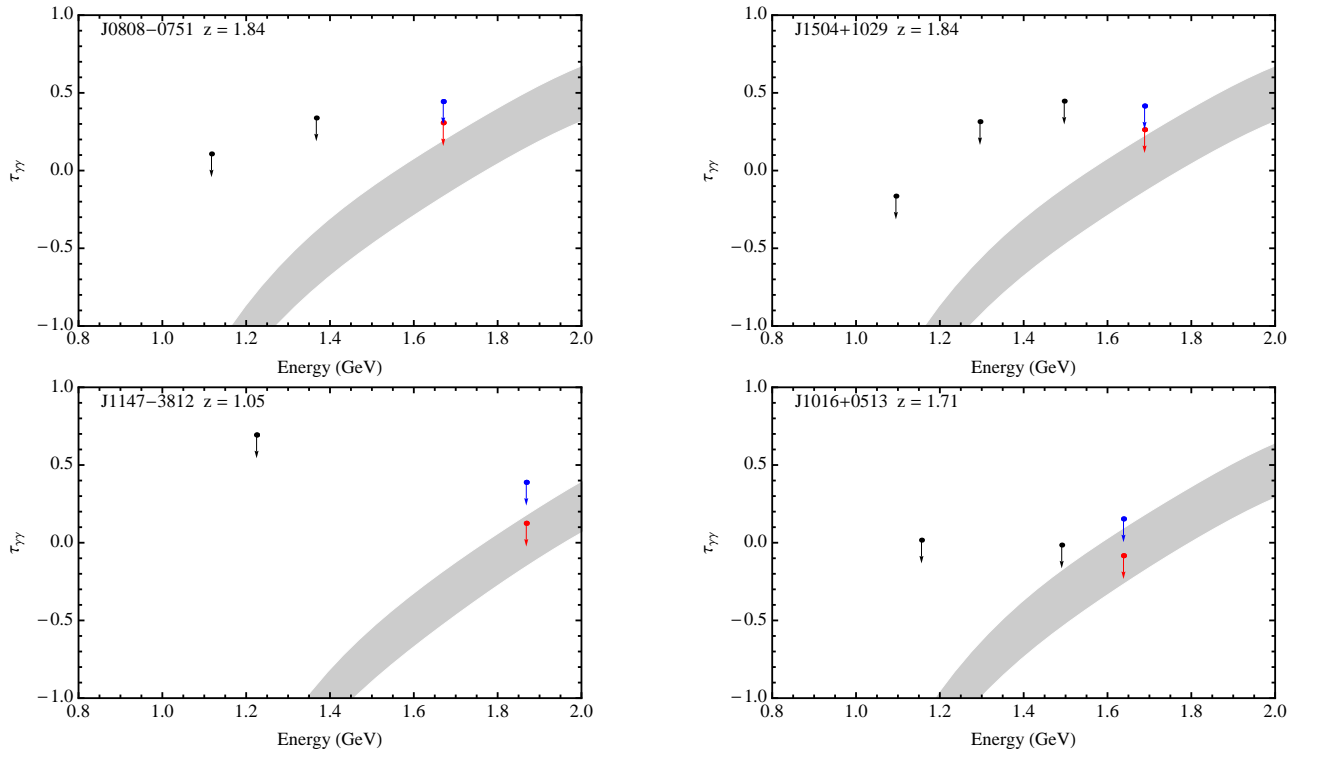


Figure 6.

REFERENCES

- Abdo, A., Ackermann, M., Ajello, M. et al. 2010, *ApJ*, 723, 1082
- Aharonian, F. et al. 2006, *Nature*, 440, 1018
- Arnouts, Schiminovich, D., Libert, O. et al 2005, *ApJ* 619, L43
- Arnouts, S. and Walcher, C. J. and Le Fèvre, O. et al. 2007, *A&A*, 476, 137
- Bertin, E., & Arnouts, S. 1996, *A&AS*, 117, 393
- Bernstein, R. A. 2007, *ApJ*, 666, 663
- Blanton, M. R., Hogg, D. W. , Bahcall, N.A. et al. 2003, *ApJ*, 592, 819
- Bouwens, R.J., Illingworth, G.D., Franx, M. & Ford, H. 2007, *ApJ*, 670, 928
- . 2008, *ApJ*, 686, 230
- Bouwens, R.J., Illingworth, G. D. Franx, M. et al. 2009, *ApJ*, 705, 936
- Bouwens, R. J., Illingworth, G. D., Oesch, P. A. et al. 2010, *ApJ*, 709, L133
- Bouwens, R. J., Illingworth, G. D., Oesch, P. et al. 2011a, *ApJ*, 737:90
- Bouwens, R. J., Illingworth, G. D., Oesch, P. et al. 2011b, *arXiv:1105.2038*
- Brammer, G. B., Whitaker, K.E., van Dokkum, P.G., Marchesini, D. et al. (2011), *ApJ*, 739, 24
- Breit, G and Wheeler, J.A. 1934, *Phys. Rev.* 46, 1087
- Bruzual, G., & Charlot, S. 2003, *MNRAS*, 344, 1000
- Budavári, T., Szalay, A.S., Charlot, S. et al. 2005, *ApJ*, 619, L31
- Bunker, A. J., Wilkins, S., Ellis, R. S. et al. 2010, *MNRAS*, 409, 855
- Burgarella, D., Pérez-González, P. G., Tyler, K. D. et al. 2006, *A&A*, 450, 69
- Capak, P., Aussel, H., Ajiki, M., et al. 2007, *ApJS*, 172, 99

- Castellano, M. Fontana, A., Grazian, A. et al. 2012, A&A540, 39
- Chary, R. & Elbaz, D. 2001, ApJ, 556, 562
- Chen, H.-W., Marzke, R.O., McCarthy, P.J. et al. 2003, ApJ, 586, 745
- Cirasuolo, M., McLure, R.J., Dunlop, J.S. et al. 2010, MNRAS, 401, 1166
- Cohen, J. G., Hsieh, S., Metchev, S., Djorgovski, S. G. & Malkan, M. 2007, AJ 133, 99
- Cucciati, O. Tresse, L., Ilbert, O. et al. 2012, A&A 539, A31
- Dahlen, T. Mobasher, B., Somerville, R. S. et al. 2005, ApJ 631, 126
- Dahlen, T. Mobasher, B., Dickinson, M. et al. 2007, ApJ 654, 172
- Dunlop, J.S., McLure, R. J., Robertson, B. E. et al. 2012, MNRAS 420, 901
- De Angelis, A., Mansutti, O., Persic, M. & Roncadelli, M. 2009 MNRAS 394, L21
- Essey, W., Kalashev, O. E., Kusenko, A. and Beacom, J. F. 2010, Phys. Rev. Letters 104, 141102
- Essey, W. & Kusenko, A. 2012, ApJ 751, L11
- Faber, S.M., Willmer, C.N.A., Wolf, C. et al. 2007, ApJ, 665, 265
- Fazio, G. G. & Stecker, F. W. 1970, Nature 226, 135
- Franceschini, A., Rodighiero, G. & Vaccari, M. 2008, A&A, 487, 837
- Gernot, M. 2011, in *Proc. XMM Science Workshop, Berlin*, article 098
- Georganopoulos, M, Fincke, J.D. & Reyes, L.C. 2010, ApJ, 714, L57
- Gialalisco, M., Dickinson, M., Ferguson, H. C. et al. 2004, ApJ, 600, L103
- Gilmore, R. C. and Madau, P., Primack, J. R., Somerville, R. S. & Haardt, F. 2009, MNRAS, 399, 1694
- Gardener, J. P., Brown, T. M. & Ferguson, H. C. 2000, ApJ, 542, L79

- González, V., Bouwens, R., Labbe, I. et al. 2011, arXiv:1110.6441
- Hathi, N. P., Ryan, R.E., Jr.; Cohen, S.H. et al. 2010, ApJ, 720, 1708
- Hauser, M. & Dwek, E. 2001, Ann. Rev. Astron. Astrophys. 39, 249
- Heath-Jones, D., Peterson, B., Colless, M. & Saunders, W. 2006, MNRAS369, 25
- Hewett, P.C., Warren, S.J., Leggett, S.K, & Hodgkin, S.T. 2006 MNRAS367, 454
- Hill, D.T., Driver, S.P., Cameron, E. et al. 2010, MNRAS 404, 1215
- Hill01 Hill, M.D. & Shanks, T. 2011, MNRAS, 414, 1875
- Ilbert, O., Lauger S., Tresse, L. et al. 2006, A&A 453, 809
- Iwata, I., Ohta, K., Tamura, N. et al. 2007, MNRAS, 376, 1557
- Jacobson, T., Liberati, S., Mattingly, D., & Stecker, F. W. 2004, Phys. Rev. Lett., 93, 021101
- Kneiske, T. M., Bretz, T., Mannheim, K. & Hartmann, D. H. 2004, A&A, 413, 807
- Kneiske, T. M. & Dole, H. 2010, A&A, 515, A19
- Leitherer, C., Ferguson, H. C., Heckman, T. M. et al. 1995, ApJ 454, L19
- Ly, C., Malkan, M. A., Treu, T., et al. 2009, ApJ, 697, 1410
- Madau, P. 1995, ApJ, 441, 18
- Madau, P. & Pozzetti, L. 2000, MNRAS 312, L9
- Magnelli, B., Elbaz, D.; Chary, R. et al. 2011, A&A, 528, A35
- Malkan, M.A. & Stecker, F.W. 1998, ApJ, 496, 13
- 2001, ApJ, 555, 641
- Marchesini, D., van Dokkum, P. Quadri, R et al. 2007, ApJ, 656, 42
- Marchesini, D., Stefanon, M., Brammer, G.B. & Whitaker, K.E. 2012, ApJ, 748, 126

- Matsuoka, Y., Ienaka, N., Kawara, K. and Oyabu, S. 2011, ApJ, 736:119
- Mattila, K. Lehtinen, K. Väisänen, P. et al. 2011, arXiv:1111.6747
- Mazin, D. & Raue, M. 2007, A&A, 471, 439
- McLure, R. J., Cirasuolo, M., Dunlop, J. S. et al. 2009, MNRAS, 395, 2196
- McLure, R. J., Dunlop, J. S., Cirasuolo, M. et al. 2010, MNRAS, 403, 960
- Oesch, P. A., Bouwens R. J., Carollo, C. M. et al. 2010 ApJ, 725, L150
- Orr, M.R, Krennrich, F. & Dwek, E. 2011, ApJ, 733, 77
- Ouchi, M., Mobasher, B., Shimasaku, K. et al. 2009, ApJ, 706, 1136
- Palatini, S., Le Fevre, Ilbert, O. et al. 2007, A&A, 463, 873
- Reddy, N. A., & Steidel, C. C. 2009, ApJ, 692, 778
- Reddy, N. A., Steidel, C.C., Pettini, M. et al. 2008, ApJS, 175, 48
- Robotham, A.S.G & Driver, S.P. 2011, MNRAS 413, 2570
- Salamon, M.H. & Stecker, F.W. 1998 (SS98), ApJ, 493, 547
- Sawicki, M., & Thompson, D. 2006, ApJ, 648, 299
- Schechter, P. 1976, ApJ, 203, 297
- Schiminovich, D., Ilbert, O., Arnouts, S. et al. 2005, ApJ, 619, L47
- Schmidt, M. 1968, ApJ, 151, 393
- Somerville, R. S., Gilmore, R. C., Primack, J. R. & Dominguez, A. 2011, arXiv:1104.0669
- Stefanon, M. & Marchesini, D. 2011, arXiv:1112.0006
- Stecker, F.W. 1969, ApJ, 157, 507
- Stecker, F.W., De Jager, O.C. & Salamon, M.H. 1992, ApJ, 390, L49
- Stecker, F.W. & De Jager, O.C. 1993, ApJ 415, L71

- Stecker, F.W. & Glashow, S. L. 2001, *Astropart. Phys.* 16, 97
- Stecker, F.W., Malkan, M.A. & Scully, S.T. 2006, *ApJ*, 648, 774
- Steidel, C. C., Adelberger, K. L.; Giavalisco, M. et al. 1999, *ApJ*, 519, 1
- Tresse, L., Ilbert, O., E. Zucca, E. et al. 2007, *A&A*, 472, 403
- Treyer, M. A., et al. 1998, *MNRAS*, 300, 303
- Wilkins, S.M., Bunker, A. J., Stanway, E. et al. 2011, *MNRAS* 417, 717
- Willott, C. J., McLure, R. J., Hibon, P. et al., [arXiv:1202.5330](https://arxiv.org/abs/1202.5330)
- Williams, R. J., Quadri, R. F., Franx, M. et al. 2009 *ApJ* 691 , 1879
- Wuyts, S., Labbe, I., Franx, M. et al. 2007 *ApJ* 655, 51
- Wyder, T. K., Treyer, M.A., Milliard, B., et al. 2005, *ApJ*, 619, L15
- Xu, C. K., Donas, J., Arnouts, S. et al. 2005, *ApJ*, 619, L11
- Yoshida, M., Shimasaku, K., Kashikawa, N. et al. 2006, *ApJ*, 653, 988